scientific reports

Check for updates

OPEN

Low intensity pulsed ultrasound alleviates synovial fibrosis in osteoarthritis via the PI3K/AKT pathway

Qing Liao[1,4], Jun Chen[2,3,4] & Gang Liu[2]✉

Previous studies have reported that low-intensity pulsed ultrasound (LIPUS) can alleviate cartilage degradation in osteoarthritis (OA). However, the functions and mechanisms of LIPUS in synovial fibrosis with OA require further study. To investigate the role of the PI3K/AKT signaling pathway in synovial fibrosis and in LIPUS treatment in synovial fibrosis, a TGF-β stimulated rat FLS cell model and a rat OA animal model based on anterior cruciate ligament transection (ACLT) and partial medial meniscectomy (MMx) were used. The results revealed that LIPUS delayed the progression of OA. Masson staining revealed that LIPUS reduced the collagen deposition of synovial tissue in OA rats. Correspondingly, immunofluorescence demonstrated that LIPUS significantly downregulated the expression of α-SMA, Col1a1 and Col3a1 in OA rats. Moreover, TGF-β stimulation upregulated fibrosis markers at the mRNA and protein levels in FLS, as well as increased phosphorylation-dependent activation of the PI3K/Akt pathway. 740Y-P was found to promote the fibrotic change of FLS induced by TGF-β, but LY294002 reduced its expression. However, LIPUS inhibits the fibrotic change and activation of the PI3K/Akt pathway in FLS under stimulation of TGF-β. In conclusion, LIPUS alleviates synovial fibrosis by blocking the PI3K/AKT pathway.

Keywords Osteoarthritis, Synovial fibrosis, Low-intensity pulsed ultrasound, PI3K/AKT signaling pathway, Synovitis, Fibroblast-like synoviocyte

Abbreviations

LIPUS	low-intensity pulsed ultrasound
OA	osteoarthritis
PI3K	phosphatidylinositol 3-kinase
AKT	Protein Kinase B
ACLT	anterior cruciate ligament transection
MMx	anterior half of medial meniscus resection
qPCR	quantitative polymerase chain reaction
WB	western blot
IL	interleukin
TNF	tumor necrosis factor
TGF	transforming growth factor
NC	normal control
DEPs	differentially expressed proteins
KEGG	kyoto encyclopedia of genes and genomes
GO	gene ontology
ELISA	enzyme-linked immunoassay
CCK8	cell counting kit 8
EdU	5-ethynyl-2'-deoxyuridine
α-SMA	alpha-smooth muscle actin
Col	collagen

[1]School of Traditional Chinese Medicine, Southern Medical University, Guangzhou 510000, China. [2]Department of Rehabilitation Medicine, Nanfang Hospital of Southern Medical University, Guangzhou 510000, China. [3]Taihe Hospital, Hubei University of Medicine, Shiyan City 442000, China. [4]Qing Liao and Jun Chen have contributed equally to this work ✉email: lg2781@smu.edu.cn

MMP	matrix metalloproteinase
SD	standard deviation
cAMP	cyclic adenosine monophosphate

Osteoarthritis (OA) is a common chronic disease that can affect the knee joint[1]. It manifests itself primarily as cartilage degeneration, synovitis, subchondral bone sclerosis, and osteophyte formation, of which synovitis is considered an important feature of OA development[2,3]. Synovitis induces synovial fibrosis and results in synovial tissue hyperplasia and joint pain[4,5]. Under pathological conditions of synovitis, synovial tissue secretes inflammatory factors, such as IL-1β and TNF-α, following stimulation, which induce proliferation and fibrotic changes in the synovial fibroblasts, ultimately leading to synovial fibrosis[5,6]. Synovial fibrosis promotes the secretion of additional inflammatory factors and collagen deposition, which further exacerbates joint pain and stiffness, impairs joint movement, and reduces the quality of patient survival[7,8]. Consequently, the controlled synovial inflammation and fibrosis represent a significant avenue for the treatment of OA.

A number of treatments are available for cartilage degeneration and synovitis of OA, including glucosamine sulfate, hyaluronic acid, non-steroidal anti-inflammatory drugs (NSAIDs), and surgical treatments such as joint replacement[9,10]. Nevertheless, the pathogenesis and treatment of synovial fibrosis in osteoarthritis remain incompletely understood[4,11]. Compared to drugs and surgery, low-intensity pulsed ultrasound (LIPUS) has been widely used as safe and non-invasive physical therapy for the treatment of joint trauma, soft tissue injuries, and other diseases by regulating the inflammatory response associated with various signaling pathways[12–15]. Some studies have shown that LIPUS is beneficial for the treatment of OA, when focused on cartilage degeneration and synovitis[12,16]. Interestingly, LIPUS improves fibrosis in the myocardium and kidney[13,15]; however, the reports involving LIPUS treatment of synovial fibrosis are limited.

Previous studies have indicated that targeting the PI3K/AKT signaling pathway inhibits fibrosis of the oral mucosa, peritoneum, and liver[17–19]. In addition, PI3K/AKT pathway inhibitors, such as GSK2126458, HEC68498, and rapamycin, are being studied or have completed clinical trials for the treatment of liver fibrosis[20]. It should be noted that inhibition of PI3K/AKT also reduced synovial inflammation and fibrosis caused by M1 polarization of synovial macrophages[21]. The above results demonstrated that inhibition of PI3K/AKT pathway can relieve synovial inflammation and fibrosis. However, in OA, it is unclear whether LIPUS can inhibit synovial fibrosis by attenuating the PI3K/AKT signaling pathway.

Therefore, we used a rat OA model established by anterior cruciate ligament transection (ACLT) combined with partial medial meniscus excision (MMx) and a TGF-β-induced rat fibroblast-like synovicytes(FLS) fibrosis model to investigate the effects of LIPUS on rat synovial fibrosis. We propose that LIPUS affects synovial fibrosis by regulating the PI3K/AKT signaling pathway.

Method

Ethical statement

All experimental protocols involving animals were reviewed and approved by the Animal Research Committee regulations of the Forevergen Medical Experiment Animal Center (No. IACUC-AEWC-F2207019). All research procedures were carried out in accordance with relevant guidelines and regulations of the Animal Care and Use Committee of the Forevergen Medical Research Animal Center. All methods are reported in accordance with ARRIVE guidelines. Eighteen male adult Sprague-Dawley rats were purchased from the Southern Medical University Experimental Animal Management Center (Guangzhou, China). These rats were housed in an appropriate temperature and humidity environment with 12 h of light and 12 h of darkness per day. Efforts were made to alleviate the suffering of rats.

Grouping of rats and establishment of an OA model

Eighteen male adult Sprague-Dawley rats (8 weeks old, 250 ± 20 g) were randomly divided into three groups: normal control (NC), osteoarthritis (OA), and LIPUS ($n = 6$). The rat OA model was established using anterior cruciate ligament transection (ACLT) combined with partial medial meniscus excision (MMx). Briefly, rats were first placed under general anesthesia by intraperitoneal injection of 2% pentobarbital (40 mg/kg, Sigma-Aldrich, St. Louis, MO, USA). The hair from the right knee joint of each rat was removed with a shaver and the area was disinfected with iodophor. We aseptically incised the knee joint capsule and dislocated the patella to expose the anterior cruciate ligament and the medial meniscus, and then cut the anterior cruciate ligament with a scalpel. The rat knee joint was then flexed 90 ° and part of the medial meniscus was removed. After surgery, the joint capsule and skin of each rat were sequentially sutured with surgical sutures and the surgical site was again disinfected with iodophor solution. In the NC group, no surgical treatment was performed. After surgery, the rats were allowed to move freely, eat (experimental rat and mouse food, Huafukang, Beijing, China), and drink water. One of the rats in the LIPUS group did not survive two weeks following the surgical procedure.

Isolation and culture of rat fibroblast-like synovicytes

Rat fibroblast-like synovicytes (FLS) were obtained from the synovial tissue of the male Sprague-Dawley rat knee joints. Rats aged 8 to 10 weeks were sacrificed by cervical dislocation and immersed in 75% alcohol for 10 min for disinfection. Ophthalmic scissors were used to cut the joint capsule and the patellar ligament of the rat knee joint. Synovial tissue is a layer of yellow-white tissue located between the patellar ligament and the joint cavity. The removed synovial tissue was washed several times in sterile PBS containing a penicillin-streptomycin solution (15140-122, Gibco, Thermo Fisher Scientific, Waltham, MA, USA). Then it was placed in 0.1% type II collagenase (17101015, Gibco) and digested for 6 to 8 h. After digestion, synovial tissue was converted into synovial fibroblasts. The digested cells were transferred to a 15-ml centrifuge tube and centrifuged for 5 min (1000 rpm). The supernatant and oil were discarded and the remaining cells were transferred to high-glucose

DMEM (10-013-CV, Corning, Corning, NY, USA) containing 10% FBS (10099141 C, Gibco) and 1% penicillin - streptomycin solution. Cells were grown in a cell culture incubator at 37 ° C and 5% CO_2.

TGF-β intervention parameters and LIPUS treatment parameters

These cells were digested and seeded in 6-well plates at a cell density of 2×10^5 cells/well and randomly divided into 3 groups: Control, TGF-β, and LIPUS. The center frequency of the 4 cm^2 transducer (LIPUSTIM® Acoustic Dynamic Therapy System, SXULTRASONIC, Shenzhen, China) is 1.5 MHz, the average intensity is 30mW/cm^2, the pulse repetition rate is 1000hz and the duty cycle is 20%, where its output acoustic power is 0.026 W. Animals and cells were treated with the same therapeutic parameters, which were selected based on previous studies[12,22].

In vitro experiments, cells were treated with 10ng/ml TGF-β (MA0623, Meilunbio, Dalian, China) to observe the effects of TGF-β on proliferation, inflammation and fibrosis. After TGF-β stimulation, ultrasound therapy was administered and ultrasound therapy was performed every 12 h, with a total of 4 times. The LIPUS simulations were conducted in a sterile environment at room temperature. LIPUS transducer was fixed at the bottom of a 6-well plate covered by acoustic gel to ensure optimal ultrasound exposure. The PI3K agonist 740 Y-P (HY-P0175, MedChemExpress, Monmouth Junction, NJ, USA) and the PI3K inhibitor LY294002 (HY-10108, MedChemExpress) at a concentration of 10μM were used to verify whether LIPUS regulates synovial fibrosis through the PI3K/Akt signaling pathway. Cell samples were collected after the treatment for qPCR, WB, and other experiments.

In vivo experiments, each rat was treated with ultrasound once a day for 20 min, beginning the first day after animal modeling and lasting 4 weeks. During treatment, the right knee joint of the rat was fixed to a specific device after approximately 100 ° flexion, the hair around the knee joint of the rats was shaved, and then a layer of coupling gel was applied between the front of the right knee joint and the transducer to ensure optimal ultrasound exposure. The distance between the transducer and the right knee joint was approximately 2–4 mm, which was fixed and kept constant in all experiments. The period of ultrasound treatment is fixed at 3–6 PM every day to ensure the stability of the intervention, while not affecting normal rest and rest of the animals. Rats were anesthetized in the afternoon of the second day after treatment and right knee joint and serum samples from rats were collected for subsequent animal experiments.

Histopathology

The right knee joint of the rat was harvested and fixed in 4% paraformaldehyde solution (SH268C, Sihe Biotechnology, Guangzhou, China) for 48 h, and then the tissue was decalcified with a decalcifying solution (G1105-500ML, Servicebio, Wuhan, China). For calcium, decalcification is continued for six to eight weeks. After decalcification, dehydration was performed using a dehydrator (ASP300S, Leica, Germany) and finally a paraffin embedding machine (TB718C, Taiwei, Wuhan, China) and a Leica microtome (HistoCore BIOCUT R, Leica, Germany) were used for embedding and sectioning. The paraffin-embedded knee tissues were cut into 5 μm sections continuously. Safranin fast green (S8884-25G, 2353-45-9, SIGMA, American), toluidine blue (G3668, Solarbio, Beijing, China), HE (1121A22, 1129A21, Leagene, Beijing, China) and Masson stain (G1340, Solarbio, Beijing, China) were used for staining according to the kit manufacturer's instructions. The Osteoarthritis Research Society International (OARSI) scoring system was used to assess the degree of cartilage degeneration in the knee joint[23]. The synovitis score and the collagen deposition score were used to evaluate knee joint synovitis and synovial fibrosis[11,24]. The above scores were classified by two independent investigators. They were aware of the grading criteria for the above stains and were blinded to the group to which each sample was assigned.

Immunohistochemistry

After tissue sections were deparaffinized and hydrated, antigen repair was performed in a microwave oven using TE9.0 antigen repair solution (G1203-250ML, Servicebio, Wuhan, China). This was followed by incubation in hydrogen peroxide solution (35000, Thermo Fisher, USA) and 10% goat serum to block endogenous peroxidase and nonspecific antigens. Tissues were incubated with primary antibodies overnight at 4 °C, followed by incubation with secondary antibodies for 1 h at 25 ± 2 °C. Finally, a DAB kit (ZLI-9018, Zhongshan Jinqiao, Beijing, China) was used to visualize antibodies in tissue sections. An optical microscope (OLYMPUS BX43, Olympus, Japan) was used to collect visual tissue images and the percentage of positive areas in the tissue was determined using ImageJ software. Five high-power fields were randomly selected from each tissue for semi-quantitative analysis. Primary antibodies: MMP13 (1:200; 18165-1-AP; proteintech; USA), Col2a1 (1:1000; 28459-1-AP; proteintech; USA), Col3a1 (1:500; 22734-1-AP; proteintech; USA). Secondary antibody: GR (SA00004-2; proteintech; USA).

Immunofluorescence

The steps prior to primary antibody incubation are similar to those of immunohistochemistry. The only difference is that immunofluorescence does not require blocking with hydrogen peroxide solution. After incubating the tissue with the primary antibody overnight at 4 °C, the fluorescent secondary antibody is incubated. It should be noted that the type and color of the secondary antibody must match the primary antibody. DAPI anti-fluorescence quenching mounting medium (S2110, Solarbio, Beijing, China) was used for sealing. Finally, a fluorescence microscope (OLYMPUS BX43, Olympus, Japan) was used to observe and record the fluorescence images, and the area percentage of positive areas was counted for comparison. Primary antibodies: α-SMA (1:1000; 14395-1-AP; proteintech; USA), Col3a1 (1:200; 22734-1-AP; proteintech; USA). Fluorescent secondary antibodies: Alexa Fluor® 488 (1:200, ab150077, abcam, UK), Alexa Fluor® 594 (1:200, ab150080, abcam, UK).

Proteomics

We collected rat abdominal aortic blood in a vacuum blood collection tube through a syringe, left it at room temperature for 30–60 min and then centrifuged at 2500 g for 15 min at 4 ° C. Then transfer the upper layer of light-yellow serum to an EP tube, add a volume of protease inhibitor corresponding to the serum volume, mix, and store quickly at -80 °C. The whole process takes no more than two hours. Proteomic detection and bioinformatics analysis were performed by Beip Bio. Three samples were selected from each group for analysis by (data-independent acquisition, DIA) DIA proteomics at Beip Biotech. The resulting data included differentially expressed protein (DEP) data between the OA group and the LIPUS group, as well as Gene Ontology (GO) functional annotation and Kyoto Encyclopedia of Genes and Genomes (KEGG) pathway enrichment data.

Enzyme-linked immunoassay (ELISA)

Blood was collected from the abdominal aorta of rats, allowed to stand at room temperature for 15 min, and then centrifuged at 2000 rpm for 15 min in a 4 °centrifuge. After centrifugation, the supernatant is stored at -80 °C until needed for the experiment. IL-6 ELISA kit (MM-0190R1, ELISA, Yancheng, China), IL-8 ELISA kit (MM-71113R1, ELISA, Yancheng, China), IL-1β ELISA kit (MM-0047R1, ELISA kit (MM-0180R1, ELISA, Yancheng, China), TNF-α ELISA kit (MM-0180R1, ELISA, Yancheng, China) to detect the expression levels of inflammatory factors in serum; PIIINP ELISA kit (MM-0039R1, ELISA, Yancheng, China), LN ELISA kit (MM-0843R1, ELISA, Yancheng, China) and HA ELISA kit (MM-0511R1, ELISA, Yancheng, China) were used to detect the expression levels of fibrosis-related proteins in serum. All procedures were performed quantitatively according to the kit manufacturer's instructions.

Cell count kit 8 (CCK8)

We use the CCK8 kit (HY-K0301, MCE, USA) to detect the viability of FLS. We seeded FLS in a 96-well plate at a cell density of 5×10^3 cells/well and incubated for 12 h to allow cells to adhere. Then, different concentrations of TGF-β were added to intervene in FLS at different time points, and 5 duplicate wells were established in each group. After intervention, 10ul of CCK8 reagent was added to each well in the dark and cells were incubated at 37 ° C for 1–4 h. The specific time is determined on the basis of the optical density. After incubation, the optical density value at a wavelength of 450 nm was detected in a microplate reader (SYNERGYHTX, BioTek, USA), and finally, the vitality of FLS was calculated based on the OD value.

EdU cell proliferation experiment

The EdU-555 cell proliferation detection kit (C0075S, Beyotime, Shanghai, China) was used to evaluate the proliferation of FLS. According to the kit instructions, cells were seeded in a 24 well plate at 100,000 cells per well. Cells were starved for 12 h in culture medium containing 1% fetal calf serum, then replaced with culture medium containing 10% fetal bovine serum for normal culture, and TGF-β was added to stimulate cells. At the same time, LIPUS was used to act on the cells, every other time every 12 h, for a total of 4 treatments of 20 min each. After preheating the prepared 2X EdU working solution to 37 °C, equal volumes are mixed with culture medium, added to the 24-well plate and incubated for 2 h. After EdU labeling of the cells, remove the medium and add 1 ml of 4% paraformaldehyde fixative to each well to fix the cells at room temperature for 15 min. After fixation, wash cells with PBS. Add 1 mL of permeabilization solution to each well and incubate at room temperature for 15 min, then add Click reaction solution for staining. Finally, cells were incubated with Hoechst 33,342 at 37 ° C for 10 min. After incubation, five field of view were randomly selected using a fluorescence microscope (OLYMPUS BX43, Olympus, Japan) for photography and recording.

Quantitative real-time polymerase chain reaction (RT-qPCR)

TRIzol reagent (NR0002, Regan Biotechnology, Beijing, China) was used to extract RNA from rat synovial fibroblasts. We used HiScript III RT SuperMix (R323-01, Novozymes, Nanjing, China) to reverse transcribe RNA to generate a cDNA template and then used the SYBR Premix Ex TaqTMII kit (RP820A, Takara, Beijing, China) on a Roche fluorescence quantitative PCR instrument (real-time quantitative polymerase chain reaction was performed on a LightCycler 96, Roche, Switzerland). According to the requirements of the reagent supplier, each group of samples was prepared in three copies. The primers are as follows:

Target gene	Forward primer	Reverse primer
GAPDH	TCCAACCCAACCCTCAACAG	GGTAACCAGGCGTCCGATAC
α-SMA	ATGCTAACAACGTCCTCTCG	CCAGCTTCGTCATACTCCTG
Col3a1	AGAGGCTTTGATGGACGCAA	GGTCCAACCTCACCCTTAGC
IL-6	CCAGTTGCCTTCTTGGGACT	CTGGTCTGTTGTGGGTGGTA
TNF-α	GGAGGGAGAACAGCAACTCC	GCCAGTGTATGAGAGGGACG

The results were normalized using GAPDH as an internal reference. The relative expression level of each gene's mRNA was calculated using the formula($2^{(-\Delta\Delta Ct)}$). Primers were purchased from Qingke Biotechnology Co., Ltd. (Beijing, China).

Western blot

We used RIPA lysis buffer (KGP702-100, KGI, Nanjing, China) containing protease inhibitors (78442, Thermo Fisher, USA) to extract proteins from synovial fibroblasts, and the BCA kit (23225, Thermo Fisher, USA) was

used to detect the concentration of collected proteins. Proteins were separated by SDS-PAGE gel and transferred to PVDF membrane (IPVH00010, Merck, Germany). After blocking with 5% skim milk (GC310001-100 g, Sevier, Wuhan, China) for 1.5 h at room temperature, the PVDF membrane was incubated with primary antibody at 4 ° C overnight. Then it was incubated with the secondary antibody for 1 h at 24 ± 2 °C, and the membrane was visualized with the chemiluminescence substrate ECL (FD8020, Ford Biotechnology, Hangzhou, China), and finally a chemical reflectometer (Tanon 5200CE, Tanon, Shanghai, China) was used. Photographing and recording protein bands. Using TUBULIN as an internal control, a relative quantitative analysis of the gray value of the target protein band was performed using ImageJ software. Primary antibodies include TUBULIN (PTM-5001, Jingjie Biotech, Hangzhou, China); α-SMA (1:6000, 14395-1-AP, Proteintech, USA); Col3a1 (1:500, 22734-1-AP, Proteintech, USA); PI3K (1:400; 20584-1-AP, Proteintech, USA); p-PI3K (1:1000; AF3241, Affinity, China); AKT (1: 6000, 60203-2-Ig, proteintech, USA); p-AKT (1:6000, 66444-1-Ig, proteintech, USA); secondary antibodies include: biotin-conjugated goat anti-rabbit IgG (H + L) (SA00004-2, proteintech, USA); biotin-conjugated goat anti-mouse IgG (H + L) (SA00004-1, proteintech, U. S).

Statistical analysis

All experiments were repeated at least three times and the results were expressed as the mean ± standard deviation (SD). Statistical analysis was performed using the GraphPad Prism software (version 8.0.1). Student's t-test was used for comparisons between two groups, and one-way analysis of variance was used for comparisons among three or more groups. When the data did not conform to a normal distribution, the paired Wilcoxon test was used for comparisons between two groups, and the paired Friedman test was used for comparisons between three or more groups, followed by the Dunn post hoc test. $p < 0.05$ indicated statistical significance. The number of replicates for all in vivo experiments was consistent with the number of animals in each group. All in vitro experiments were repeated three times.

Results

LIPUS delays the progression of OA

To determine the role of LIPUS in OA, we performed histopathology to evaluate knee cartilage lesions in OA rats after LIPUS treatment. In particular, LIPUS treatment resulted in a significantly lower OA score than OA, characterized by more chondrocytes, less cartilage erosion, and loss of proteoglycans [Fig. 1a–b, Supplementary Fig. 1]. We then examined the effects of LIPUS on cartilage metabolism, LIPUS treatment reversed the increase in MMP13 expression and the decrease in type 2 collagen a1 (Col2a1) levels at 4 weeks after ACLT + MMx surgery [Fig. 1c–f]. And compared to OA, low levels of synovial hyperplasia and less inflammatory cell infiltration were observed in the synovial tissue of OA rats treated with LIPUS, combined with lower synovitis scores at 4 weeks after surgery [Fig. 1g–h]. In addition, the results of the ELISA revealed that LIPUS inhibited the expression of inflammatory factors, including IL-1β, IL-6, IL-8, and TNF-α, in serum collected from the abdominal aortas of rats with OA [Supplementary Fig. 2a-d]. These findings suggested that LIPUS can improve articular cartilage lesions, relieve synovitis, and synovial hyperplasia, which can delay the progression of OA.

LIPUS relieves synovial fibrosis in OA rats

To determine the effect of the LIPUS intervention on synovial fibrosis in rats. First, we measured the expression of the fibrotic proteins, LN, HA, and PIII-NP, in the serum of the abdominal aortas of rats by ELISA. The results indicated that the LIPUS intervention significantly decreased the levels of fibrotic proteins in the serum of OA rats [Supplementary Fig. 3a–c]. Regarding histomorphology, Masson staining revealed that collagen deposition in the synovial tissue of OA rats decreased after LIPUS treatment, thereby inhibiting synovial fibrosis [Fig. 2a, b]. Synovitis, as one of the main pathological manifestations of osteoarthritis, is closely related to fibrosis[25]. Therefore, we analyzed the correlation between synovitis scores and the percentage of synovial collagen volume fraction in rats with OA. The R values were 0.8158, indicating a positive correlation between the degree of synovitis and the fraction of synovial collagen volume [Fig. 2c]. Subsequently, we measured the expression of fibrotic proteins α-SMA and Col3a1 in synovial tissue by immunofluorescence. α-SMA and Col3a1 expression was significantly reduced in the LIPUS group compared to that in the OA group [Fig. 2d–g]. Thus, LIPUS ameliorated synovial fibrosis in OA rats.

Identification of the synovial fibrosis-related protein with and without LIPUS through proteomics

To investigate the specific target of action of LIPUS for synovial fibrosis, we performed proteomic analysis of serum from the abdominal aorta of rats in the OA group and the LIPUS group. After quality control (QC) of the proteomics data [Fig. 3a], there were 61 up-regulated proteins and 87 down-regulated proteins, respectively [Fig. 3b]. Among them, we present the top 20 significantly differentiated proteins, such as the serine protease inhibitor A11(Serpina11), type 3 collagen a1(Col3a1) and calmodulin 1 (Calm1), etc. [Figure 3c]. Additionally, the volcano diagram displays differentially expressed proteins that are significantly up- or down-regulated. One of these proteins is Col3a1, which is associated with synovial fibrosis [Fig. 3d]. To verify the expression of Col3a1 in vivo, we measured the expression of the fibrotic protein Col3a1 in rat synovial tissue using immunohistochemistry. Col3a1 expression was significantly reduced in the LIPUS group compared to the OA group [Fig. 3e-f]. The results demonstrated that LIPUS has a down-regulating effect on the fibrosis-related protein Col3a1.

LIPUS inhibits TGF-β-induced proliferation, inflammation and fibrosis of FLS

Next, we want to confirm whether LIPUS can hinder TGF-β-induced proliferation, inflammation and fibrotic change of FLS. First, we conducted in vitro experiments to identify the optimal conditions for TGF-β stimulation

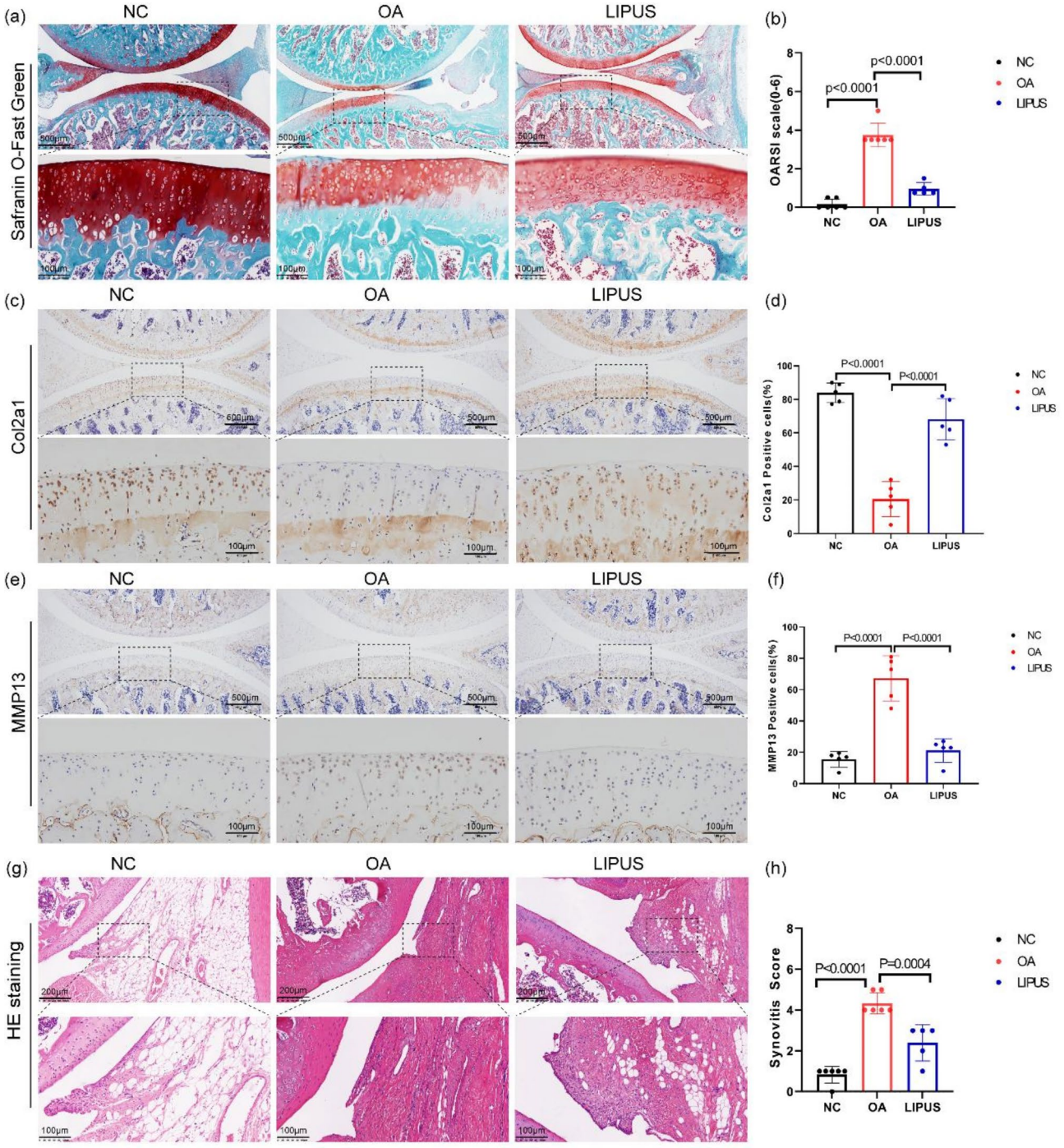

Fig. 1. LIPUS delays the progression of OA in rats. (**a**) Safranin fast green staining of knee joint cartilage from rats in the NC, OA and LIPUS groups. Scale bar: 500 μm, 100 μm. (**b**) Cartilage degeneration evaluated with the OARSI scoring system. (**c**–**f**) Immunohistochemistry (IHC) staining and quantification of anabolic and catabolic indicators, Col2a1 and MMP13, in the knee joint cartilage from rats in the NC, OA and LIPUS groups. Scale bar: 500 μm, 100 μm. (**g**, **h**) Hematoxylin and eosin (H&E) staining and synovitis scores of rats in the NC, OA, and LIPUS groups. Scale bar: 200 μm, 100 μm. The specific *P* values are presented in the graph.

of rat synovial fibroblast proliferation. CCK8 was used to detect FLS cell proliferation induced by TGF-β at five concentrations (0, 1, 5, 10, and 20ng/ml). The proliferation of FLS cells induced by TGF-β at different times was measured at the optimal concentration of 10ng/ml [Supplementary Fig. 4a]. The results indicated that cell proliferation was evident at the 48-hour time point [Supplementary Fig. 4b]. And the results of the EdU proliferation experiment indicated that TGF-β induced FLS proliferation [Fig. 4a-b]. Furthermore, the qPCR results demonstrated that TGF-β enhanced the expression of inflammatory genes in FLS [Fig. 4c]. On the other

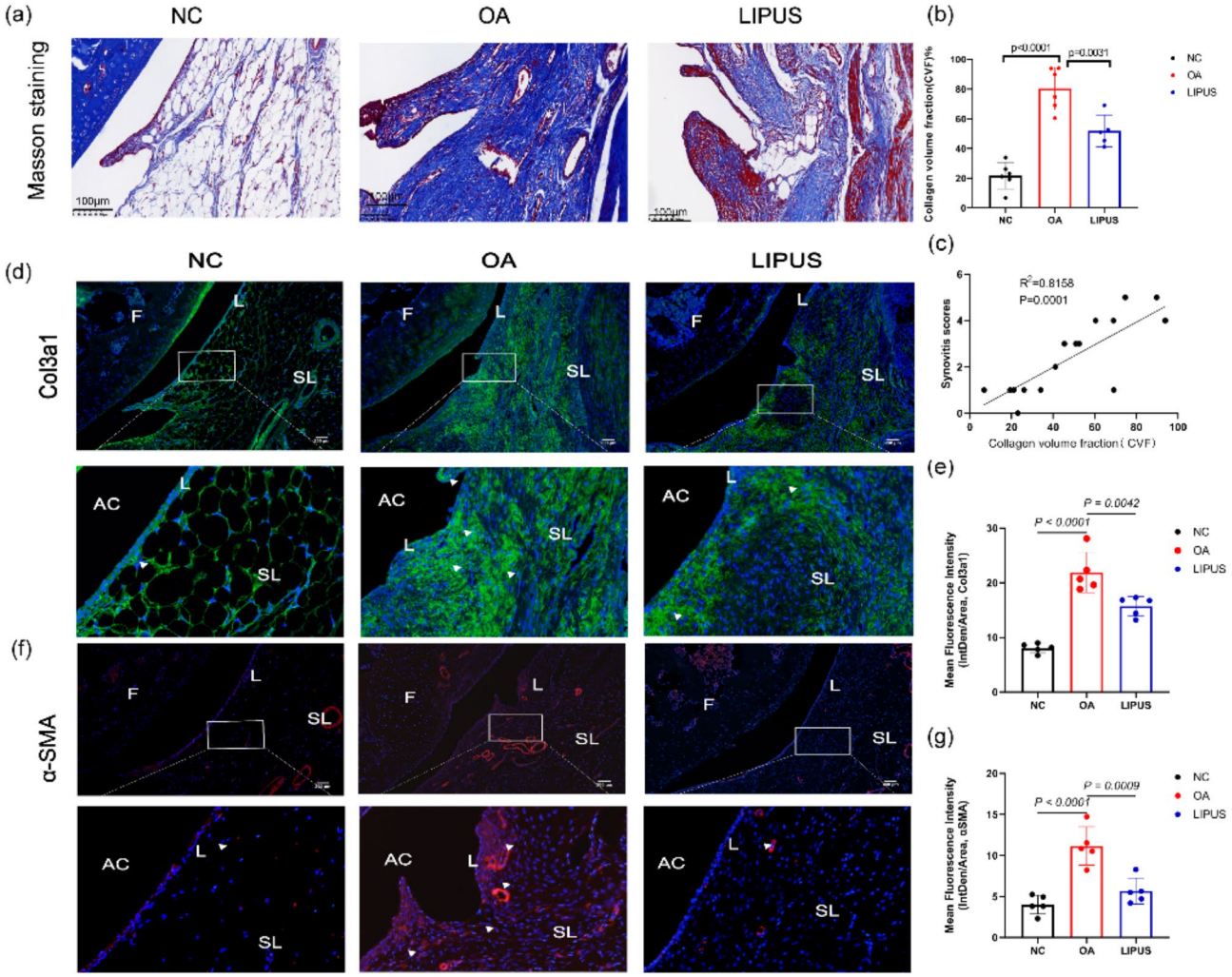

Fig. 2. LIPUS relieves synovial fibrosis in OA rats. (**a**, **b**) Masson's staining and collagen volume fraction of synovial tissues of rats in the NC, OA and LIPUSA groups. Scale bar: 100 μm. (**c**) Correlation between the degree of synovitis and the fraction of collagen volume of synovial tissue. (**d**, **e**) Immunofluorescence staining (IF) and quantification of Col3a1 in synovial tissue of rats in the NC, OA and LIPUS groups. Scale bar: 200 μm. (**f**, **g**) Immunofluorescence staining (IF) and quantification of α-SMA in synovial tissue from rats in the NC, OA and LIPUSA groups. Scale bar: 200 μm. The specific P values are presented in the graph. F-femur, L- lining layer, SL- sub-lining layer, AC- articular cavity.

hand, we further clarify that TGF-β upregulated fibrosis-related genes and proteins, such as α-SMA, Col3a1, and Col1a1[Figure 4d-g]. In brief, TGF-β can induce the proliferation, inflammation and fibrotic phenotype of FLS.

Moreover, the results of the EdU proliferation experiment indicate that LIPUS treatment inhibited TGF-β-induced FLS proliferation [Fig. 4a-b]. Additionally, the qPCR results indicated that LIPUS treatment resulted in the downregulation of TNF-α and IL-6 expression in FLS [Fig. 4c]. Together with this, western blot and qPCR analyze revealed that LIPUS inhibited the expression of fibrotic molecules of FLS [Fig. 4h-k]. These results indicate that TGF-β induces proliferation, inflammation and fibrotic changes of FLS, while LIPUS inhibits TGF-β-induced proliferation, inflammation and fibrotic changes of FLS. Thus, LIPUS can inhibit TGF-β-induced proliferation, inflammation and fibrosis in FLS.

PI3K/AKT pathway promotes TGF-β-induced fibrosis of FLS

The potential for the PI3K/AKT pathway to promote TGF-β-induced fibrotic change in FLS remains uncertain. Therefore, to elucidate the role of the PI3K/AKT pathway in TGF-β-induced fibrotic change of FLS, 740 Y-P, and LY294002 were used to activate and inhibit this pathway, respectively. Western blot analysis was used to detect the expression of pathway proteins. The results indicated that the expression of the p-PI3K and p-AKT proteins was up-regulated after treatment of synovial fibroblasts with 740 Y-P, while the expression of the p-PI3K and p-AKT proteins was down-regulated after treatment of FLS with LY294002 [Fig. 5a–c].

Next, we measured the expression of fibrosis proteins in TGF-β-induced FLS. Treatment with 740 Y-P significantly increased the expression of fibrosis proteins, α-SMA and Col3a1, in FLS. In contrast, LY294002

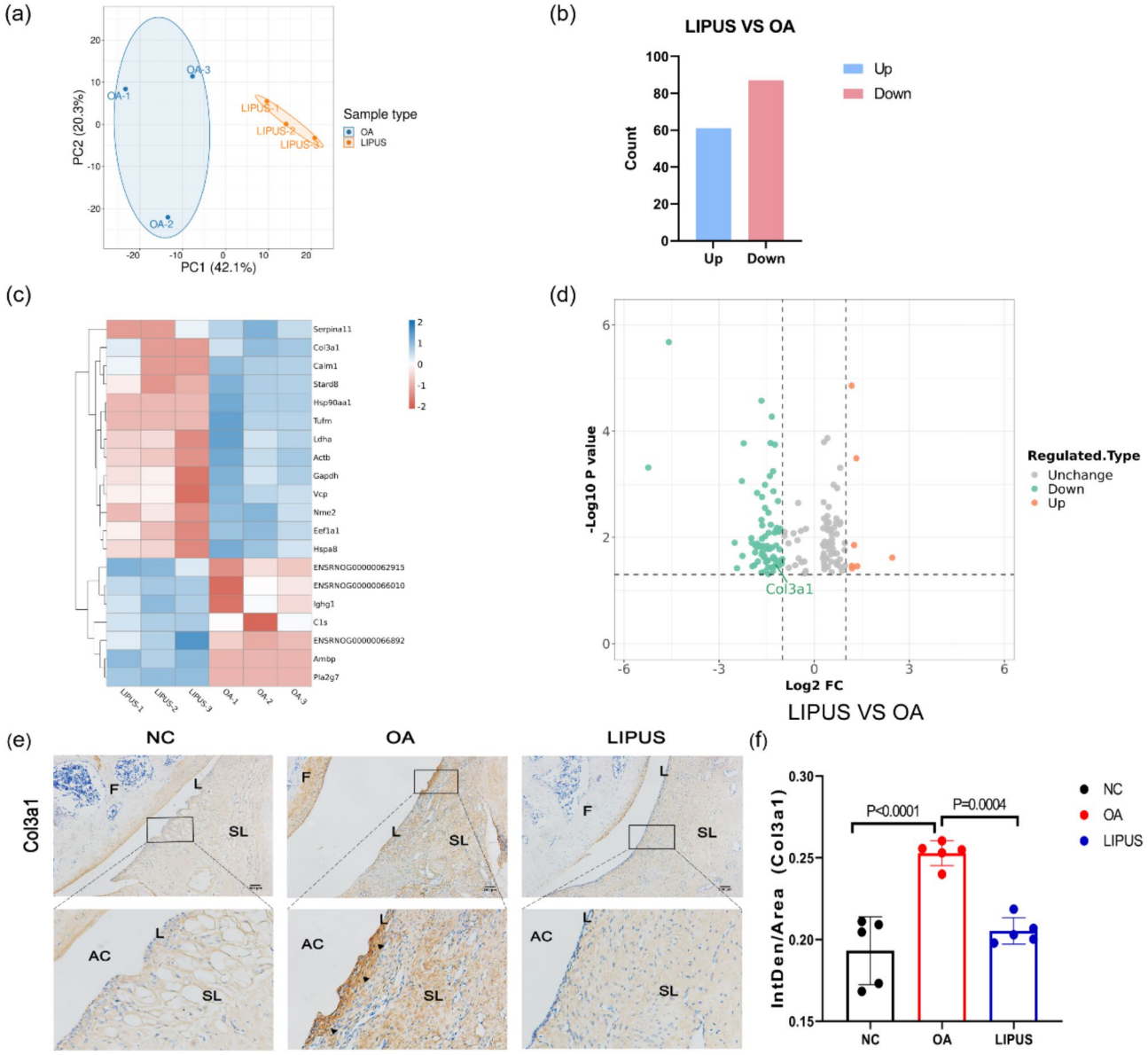

Fig. 3. Identification of the synovial fibrosis-related protein with and without LIPUS through proteomics. (**a**) PCA quality control chart showing the serum proteomics results of rats in the OA and LIPUS groups. (**b**) The number of differential proteins was up-regulated or down-regulated. (**c**) The heat map displayed the top 20 differential proteins. (**d**) The volcano plot shows the trend of Col3a1 expression in the OA and LIPUS groups. (**e**, **f**) Immunohistochemical staining (IHC) and quantification of Col3a1 in synovial tissue of rats in the NC, OA and LIPUSA groups. Scale bar: 200 μm. The specific P values are presented in the graph. F-femur, L- lining layer, SL- sub-lining layer, AC- articular cavity.

reduced their expression [Fig. 5d–f]. As a consequence, PI3K/AKT signaling pathway can promote TGF-β-induced fibrotic phenotype of FLS.

LIPUS reduces synovial fibrosis via PI3K/AKT/Col3a1 axis

Next, we explored whether LIPUS relieved synovial fibrosis by inhibiting PI3K/AKT signaling pathway. To further assess the effect of LIPUS on the PI3K/AKT signaling pathway, LIPUS was applied to TGF-β-induced FLS, and western blot analysis was used to measure the related protein expression level of PI3K/AKT signaling pathway. The results indicated that the expression of PI3K/AKT pathway was significantly increased in TGF-β-induced FLS, while LIPUS inhibited PI3K/AKT pathway [Fig. 6a–c]. Furthermore, immunohistochemical analysis of OA synovium revealed that LIPUS suppressed the expression of p-AKT protein [Supplementary Fig. 5a-b]. The protein expression of Col3a1 increased significantly after TGF-β induction, which was reversed by LIPUS [Fig. 6d-f]. Thus, the PI3K/AKT/Col3a1 axis is an important pathway for the treatment of synovial fibrosis with LIPUS.

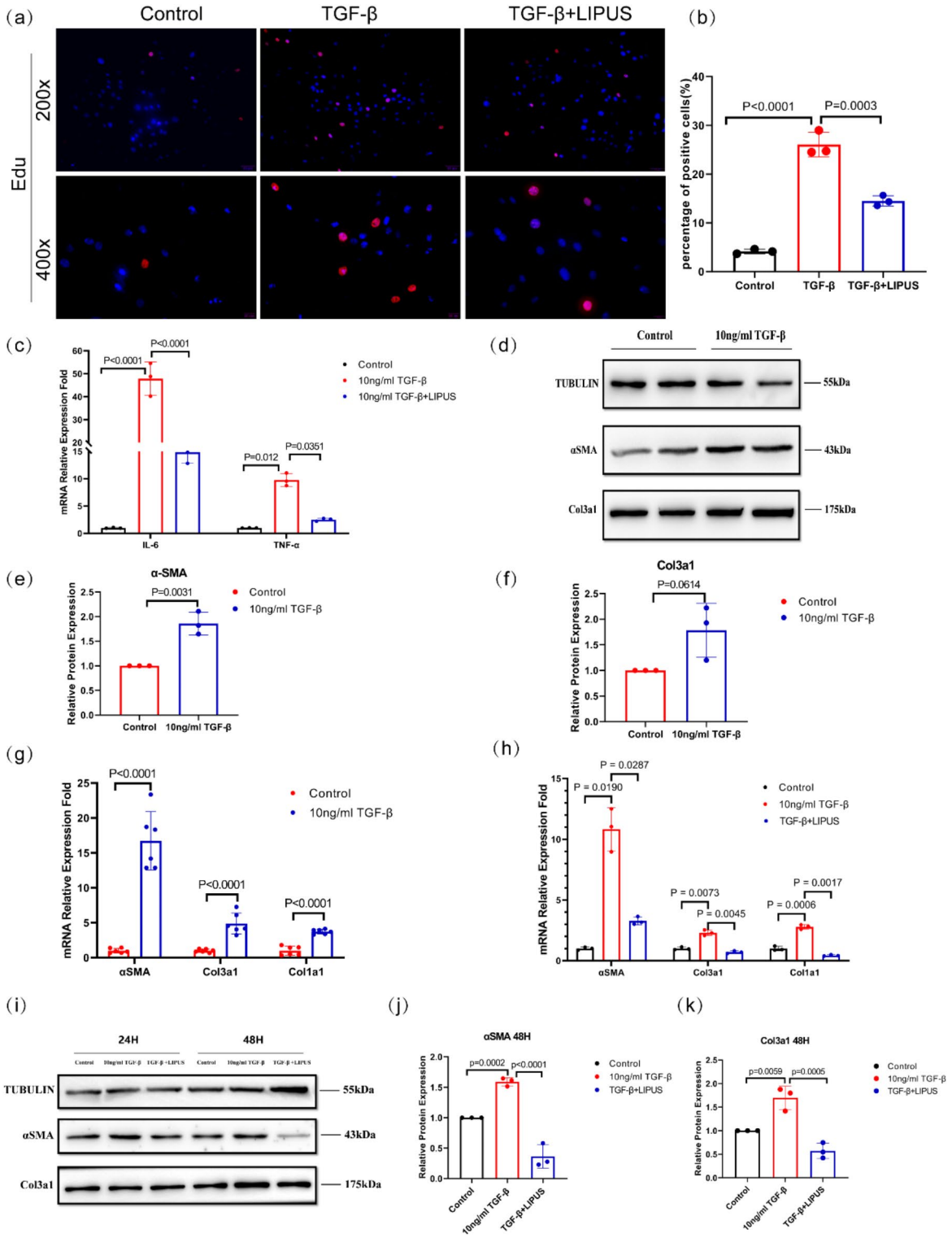

Fig. 4. LIPUS inhibits TGF-β-induced proliferation, inflammation and fibrosis of FLS. (**a**, **b**) Effect of LIPUS on TGF-β-induced proliferation of FLS. $n = 3$; (**c**) Relative mRNA levels of IL-6 and TNF-α in FLS under the effects of TGF-β and LIPUS. $n = 3$; (**d**-**f**) Protein expression of αSMA and Col3a1 in FLS under the influence of TGF-β. $n = 3$; Original blots are presented in Supplementary Fig. 6; (**g**) Relative expression of αSMA, Col3a1, and Col1a1 mRNA in FLS under the influence of TGF-β. $n = 3$; (**h**) Relative mRNA levels of αSMA, Col3a1, and Col1a1 mRNA in rat synovial fibroblasts under the effects of TGF-β and LIPUS. $n = 3$; (**i**-**k**) Protein expression of αSMA and Col3a1 was evaluated after LIPUS treatment in FLS induced by TGF-β. $n = 3$; Original blots are presented in Supplementary Fig. 7; The specific P values are presented in the graph.

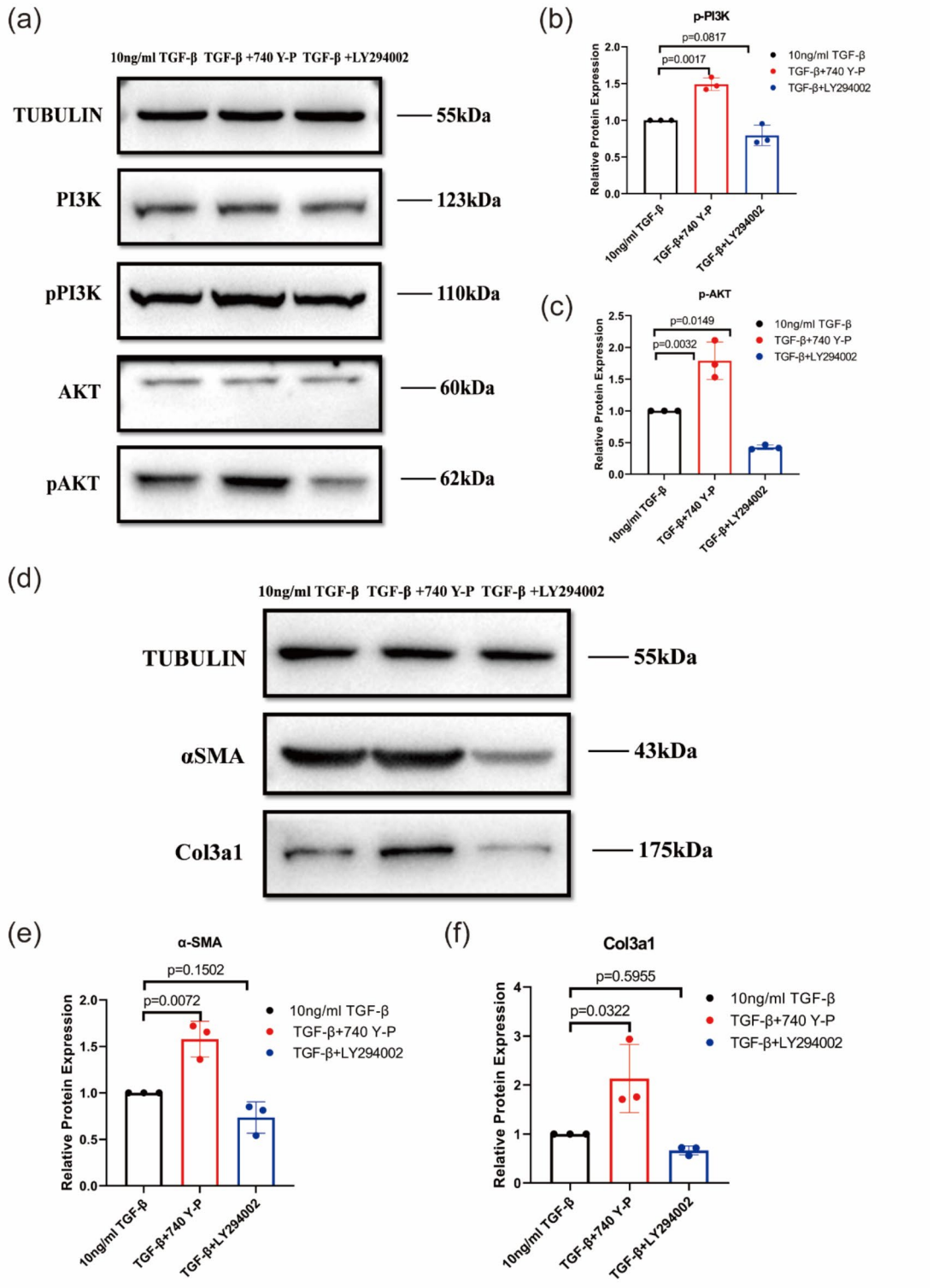

Fig. 5. PI3K/AKT pathway promotes TGF-β-induced fibrotic change of FLS. (**a**-**c**) Activation and inhibition of the PI3K/AKT signaling pathway in TGF-β-induced FLS by a PI3K agonist (740 YP) and inhibitor (LY294002). $n = 3$; Original blots are presented in Supplementary Fig. 8; (**d**-**f**) 740 YP induced the expression of fibrotic proteins, αSMA and Col3a1, in TGF-β-induced FLS, whereas they were down-regulated by LY294002. $n = 3$; Original blots are presented in Supplementary Fig. 9; The specific P values are presented in the graph.

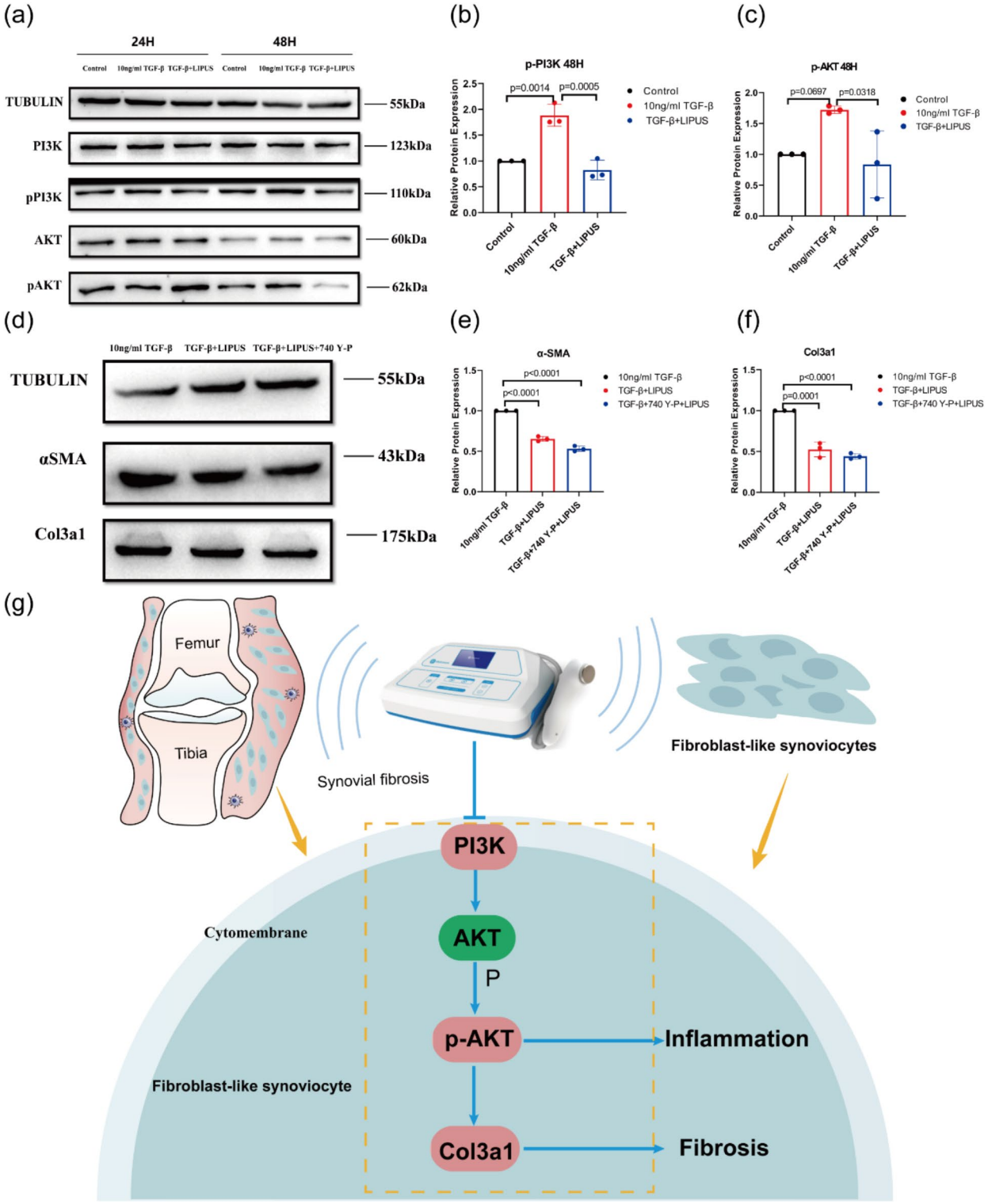

Fig. 6. LIPUS ameliorates synovial fibrosis by regulating PI3K/AKT pathway. (**a**-**c**) LIPUS inhibits the expression of p-PI3K and p-AKT proteins at 24 and 48 h of TGF-β-induced FLS. $n = 3$; Original blots are presented in Supplementary Fig. 10; (**d**-**f**) During LIPUS, the profibrotic effect of 740 Y-P on TGF-β-induced FLS was inhibited. $n = 3$; Original blots are presented in Supplementary Fig. 11; (**g**) LIPUS ameliorated synovial fibrosis by inhibiting PI3K/AKT pathway and expression of Col3a1. The specific P values are presented in the graph.

To further corroborate these results, LIPUS was used to intervene in TGF-β-induced FLS following the addition of 740 Y-P. The results indicated that LIPUS significantly inhibited the activation effect of this PI3K agonist on this pathway [Fig. 6d–f]. Inhibition of the PI3K/AKT signaling pathway has been demonstrated to inhibit fibrotic changes in FLS. Our findings indicated that LIPUS ameliorated synovial fibrosis by inhibiting the PI3K/AKT/Col3a1. The potential mechanism of action of LIPUS on synovial fibrosis in OA is presented in Fig. 6g.

Discussion

Synovial fibrosis is one of the main pathological changes of OA and exacerbates its malignant progression[26,27]. Besides, synovial fibrosis is considered one of the primary factors affecting joint motion and quality of life, and is characterized by the excessive production of extracellular matrix components and αSMA expression[5,28,29]. Currently, there are clinical treatments for cartilage degeneration, synovial inflammation, and joint effusion[30,31]. However, limited studies have addressed the treatment and causes of synovial fibrosis. It is therefore imperative that reliable and effective therapies for synovial fibrosis in OA are developed. As a non-invasive, safe and effective treatment method, LIPUS has been widely used for treating bone and joint diseases[32,33]. Previous studies have indicated that LIPUS exerts a chondroprotective effect[12,34].We also found that LIPUS could alleviate cartilage degeneration in OA rats. In summary, these results indicated the beneficial effects of LIPUS in the rat with OA. Therefore, we used LIPUS to treat rats with OA and TGF-β-induced FLS and examined its effects on synovial fibrosis. The results indicated that LIPUS inhibits synovial fibrosis of OA. Specifically, inhibition of synovial fibrosis by LIPUS occurs via the PI3K/AKT/Col3a1 axis. These findings provide a rationale for studying the mechanism and treatment methods of synovial fibrosis.

In the surgically induced OA rat model, pathological changes in synovial tissue were more pronounced 2–4 weeks after surgery[35]. In the present study, 4 weeks after surgical induction, there was a notable increase in synovitis and collagen deposition in synovial tissue, as well as fibrotic proteins such α-SMA and Col3a1. It is worth noting that inflammation can cause an increase in collagen secretion, which leads to more severe fibrosis[4,36]. Our results suggested that the severity of synovitis is positively correlated with the degree of collagen deposition in synovial fibrosis. As a result, synovitis may contribute to synovial fibrosis. However, the administration of LIPUS was observed to have a significant inhibitory effect on synovial inflammation and fibrosis. In a word, LIPUS may suppresses synovitis and further reduces synovial fibrosis.

However, prior research has suggested that LIPUS is an effective intervention for the treatment of renal and cardiac fibrotic lesions[13,15]. Additionally, LIPUS has been demonstrated to regulate the function of FLS and chondrocytes in OA[12,22,37]. The results of these studies have indicated that the inhibition of synovial fibrosis by LIPUS may be a comprehensive effect. Similarly, our study investigated that LIPUS is capable of inhibiting synovial fibrosis. In order to ascertain the precise target of LIPUS in synovial fibrosis of OA, we conducted proteomic sequencing on the serum of two groups of rats: OA and LIPUS. In this study, some proteins demonstrated a notable increase in the OA group, while a decline was observed in the LIPUS group, including the Col3a1 protein, a marker of fibrosis. On the basis of proteomics, we verified LIPUS downregulated expression Col3a1 protein in synovial tissue by using IHC, which provided more sufficient evidence for subsequent studies. These findings indicated that LIPUS exerts a direct inhibitory effect on synovial fibrosis. FLS are the principal cells involved in synovial fibrosis. Moreover, the function of LIPUS varies between fibroblasts in different tissues. In periodontal ligament fibroblasts, LIPUS suppressed inflammation and promoted BMP9-induced osteogenesis[38]. In cardiac fibroblasts, LIPUS ameliorated cardiac fibrosis by alleviating inflammation via a caveolin-1-dependent pathway[13]. It can be reasonably deduced that LIPUS may play a different role in different tissues and cells. Consequently, it is imperative to investigate the cell-specific effect of LIPUS in synovial fibrosis.

In response to prolonged injury, inflammation, or mechanical stress, fibroblasts can undergo a phenotypic transformation into myofibroblasts, which are characterized by α-SMA expression, collagen-rich extracellular matrix synthesis, and fibroblast proliferation[8,39]. As a result, the phenotypic alterations observed in FLS in OA are predominantly attributed to their differentiation into myofibroblasts, which in turn gives rise to an excessive production and secretion of extracellular matrix components. This process induces synovial hyperplasia, hypertrophy, and extensive fibrosis, which in turn manifest clinically as joint stiffness and pain[7]. Previous studies have shown that microRNA-27b-3p, cAMP, and pirfenidone inhibit the expression of αSMA and Col3a1 in the synovium, thereby relieved synovial fibrosis[11,26,40].The present study demonstrated that α-SMA expression was significantly increased in ACLT + MMx-induced synovial tissues of OA rats and TGF-β-induced FLS. However, LIPUS administration resulted in a reduction in α-SMA expression in both models. These findings suggest that LIPUS may alleviate synovial fibrosis by inhibiting the transformation of FLS into myofibroblasts.

It is widely acknowledged that transforming growth factor-β (TGF-β) plays a pivotal role in collagen deposition during the process of fibrosis[41]. Prior research has demonstrated that TGF-β induced inflammation and fibrosis of FLS[29]. The findings of our study also indicated that not only were fibrotic proteins in FLS significantly upregulated in response to TGF-β stimulation, but also that there was a notable increase in the levels of proliferation and inflammation of FLS. Nevertheless, LIPUS has been shown to reverse these alterations. These findings suggest that LIPUS can effectively inhibit proliferation, inflammation and fibrosis of FLS. However, it is not yet clear whether the specific underlying mechanism of LIPUS relieves synovial fibrosis.

Interestingly, targeting the PI3K/AKT signaling pathway inhibited fibrosis in the heart[42]. Furthermore, inhibition of the PI3K/AKT pathway has been used to treat pulmonary fibrosis and liver fibrosis[43,44]. Targeting the PI3K/AKT pathway may thus be a viable strategy for inhibiting fibrosis. The study also found that inhibiting the PI3K/AKT pathway could reduce fibrosis in rat synovial fibroblasts. However, LIPUS has been suggested to exert disparate effects on diverse tissues and cells through its regulation of the PI3K/AKT pathway. In OA, LIPUS inhibited cartilage matrix breakdown by inhibiting the integrin-FAK-PI3K/Akt signaling pathway[45]. It has been indicated that LIPUS alleviated neuronal injury by inhibiting the PI3K/Akt/NF-κB pathway[46].Previous

reports have shown that LIPUS promoted the proliferation of human bone marrow-derived mesenchymal stem cells by the activation of the PI3K/AKT pathway[47]. It can be concluded that LIPUS is capable of regulating the PI3K/AKT signaling pathway directly. Similarly, our findings indicated that LIPUS inhibits the activation of the PI3K/AKT pathway in FLS. The activation of the PI3K/AKT pathway has been demonstrated to promote fibrosis of FLS. The addition of PI3K agonists to TGF-β-induced FLS in the presence of LIPUS resulted in a notable reduction in the promotion of fibrosis by PI3K agonists. This further corroborates the hypothesis that LIPUS exerts its anti-fibrotic effects by suppressing the activation of the PI3K/AKT signaling pathway.

As previously stated, FLS in OA can undergo a phenotypic transformation into myofibroblasts, which are characterized by α-SMA expression and collagen-rich extracellular matrix synthesis. Nevertheless, the activation of the PI3K/AKT signaling pathway was observed to result in an increased expression of α-SMA and Col3a1 in FLS, whereas the inhibition of the pathway was found to result in a decreased expression of both. It can thus be postulated that LIPUS may potentially inhibit the transformation of FLS into myofibroblasts by regulating the PI3K/AKT signaling pathway, which in turn inhibits synovial fibrosis.

Eventually, we found that the PI3K/AKT signaling pathway promoted the fibrosis of FLS and LIPUS alleviated synovial fibrosis in OA rats, in part, through the PI3K/AKT signaling pathway. The study presents a theoretical foundation for the clinical use of LIPUS in the treatment of OA and offers novel insights into its mechanism and effective treatment. Although our study demonstrated for the first time that LIPUS attenuates synovial fibrosis by inhibiting the PI3K/AKT pathway, it still has some limitations. Firstly, further studies are necessary to identify additional targets of the PI3K pathway in synovial fibrosis. Secondly, to elucidate the mechanism of action of LIPUS, the investigation of the TGF-β-induced PI3K/AKT signaling pathway was confined to FLS in this study. However, it is important to note that other cytokines, such as lipopolysaccharide (LPS) and TNF-α, have been observed to induce fibrosis as well. Therefore, in future studies, we may explore the potential of LIPUS to target additional signaling pathways associated with synovial fibrosis.

Conclusions

In conclusion, our study demonstrates for the first time that synovial fibrosis is inhibited following the inhibition of the PI3K/AKT pathway. Furthermore, LIPUS inhibits synovial fibrosis in part via the PI3K/AKT/Col3a1 axis, thereby exerting a beneficial effect.

Data availability

The data that support the findings of this study are available from the corresponding author upon reasonable request. The proteomics datasets have been uploaded to PRIDE repository with the dataset identifier PXD061090.

Received: 14 August 2024; Accepted: 27 February 2025
Published online: 20 March 2025

References

1. Yao, Q. et al. Osteoarthritis: pathogenic signaling pathways and therapeutic targets. *Signal. Transduct. Target. Ther.* **8**, 56 (2023).
2. De Roover, A., Escribano-Núñez, A., Monteagudo, S. & Lories, R. Fundamentals of osteoarthritis: inflammatory mediators in osteoarthritis. *Osteoarthr. Cartil.* **31**, 1303–1311 (2023).
3. Abramoff, B., Caldera, F. E. & Osteoarthritis Pathology, diagnosis, and treatment options. *Med. Clin. North. Am.* **104**, 293–311 (2020).
4. Deroyer, C. et al. CEMIP (KIAA1199) regulates inflammation, hyperplasia and fibrosis in osteoarthritis synovial membrane. *Cell. Mol. Life Sci.* **79**, 260 (2022).
5. Zhang, L. et al. Synovial fibrosis involvement in osteoarthritis. *Front. Med. (Lausanne).* **8**, 684389 (2021).
6. Scanzello, C. R. & Goldring, S. R. The role of synovitis in osteoarthritis pathogenesis. *Bone* **51**, 249–257 (2012).
7. Remst, D. F. G., Davidson, B., van der Kraan, P. M. & E. N. & Unravelling osteoarthritis-related synovial fibrosis: a step closer to solving joint stiffness. *Rheumatol. (Oxford).* **54**, 1954–1963 (2015).
8. Schuster, R., Rockel, J. S., Kapoor, M. & Hinz, B. The inflammatory speech of fibroblasts. *Immunol. Rev.* **302**, 126–146 (2021).
9. Bannuru, R. R. et al. OARSI guidelines for the non-surgical management of knee, hip, and polyarticular osteoarthritis. *Osteoarthr. Cartil.* **27**, 1578–1589 (2019).
10. Glyn-Jones, S. et al. *Osteoarthr. Lancet* **386**, 376–387 (2015).
11. Wei, Q. et al. Pirfenidone attenuates synovial fibrosis and postpones the progression of osteoarthritis by anti-fibrotic and anti-inflammatory properties in vivo and in vitro. *J. Transl Med.* **19**, 157 (2021).
12. Liao, Q. et al. Low-intensity pulsed ultrasound promotes Osteoarthritic cartilage regeneration by BMSC-derived exosomes via modulating the NF-κB signaling pathway. *Int. Immunopharmacol.* **97**, 107824 (2021).
13. Zhao, K. et al. Low-intensity pulsed ultrasound ameliorates angiotensin II-induced cardiac fibrosis by alleviating inflammation via a caveolin-1-dependent pathway. *J. Zhejiang Univ. Sci. B.* **22**, 818–838 (2021).
14. Zhang, Z. C. et al. Low-intensity pulsed ultrasound promotes spinal fusion by regulating macrophage polarization. *Biomed. Pharmacother.* **120**, 109499 (2019).
15. Aibara, Y. et al. Daily Low-intensity pulsed ultrasound ameliorates renal fibrosis and inflammation in experimental hypertensive and diabetic nephropathy. *Hypertension* **76**, 1906–1914 (2020).
16. Feltham, T., Paudel, S., Lobao, M., Schon, L. & Zhang, Z. Low-Intensity pulsed ultrasound suppresses synovial macrophage infiltration and inflammation in injured knees in rats. *Ultrasound Med. Biol.* **47**, 1045–1053 (2021).
17. Jia, M. et al. Inhibition of PI3K/AKT/mTOR signalling pathway activates autophagy and suppresses peritoneal fibrosis in the process of peritoneal Dialysis. *Front. Physiol.* **13**, 778479 (2022).
18. Zhang, W. S. et al. S100a16 deficiency prevents hepatic stellate cells activation and liver fibrosis via inhibiting CXCR4 expression. *Metabolism* **135**, 155271 (2022).
19. Wang, J. et al. The circEPSTI1/mir-942-5p/LTBP2 axis regulates the progression of OSCC in the background of OSF via EMT and the PI3K/Akt/mTOR pathway. *Cell. Death Dis.* **11**, 682 (2020).
20. Liu, X. et al. Ginsenoside Rg3 promotes regression from hepatic fibrosis through reducing inflammation-mediated autophagy signaling pathway. *Cell. Death Dis.* **11**, 454 (2020).
21. Yan, J. et al. Nintedanib ameliorates osteoarthritis in mice by inhibiting synovial inflammation and fibrosis caused by M1 polarization of synovial macrophages via the MAPK/PI3K-AKT pathway. *FASEB J.* **37**, e23177 (2023).

22. Zhang, B. et al. SQSTM1-dependent autophagic degradation of PKM2 inhibits the production of mature IL1B/IL-1β and contributes to LIPUS-mediated anti-inflammatory effect. *Autophagy* **16**, 1262–1278 (2020).
23. Gerwin, N., Bendele, A. M., Glasson, S. & Carlson, C. S. The OARSI histopathology initiative - recommendations for histological assessments of osteoarthritis in the rat. *Osteoarthr. Cartil.* **18** (Suppl 3), S24–34 (2010).
24. Krenn, V. et al. Synovitis score: discrimination between chronic low-grade and high-grade synovitis. *Histopathology* **49**, 358–364 (2006).
25. Robinson, W. H. et al. Low-grade inflammation as a key mediator of the pathogenesis of osteoarthritis. *Nat. Rev. Rheumatol.* **12**, 580–592 (2016).
26. Tavallaee, G. et al. Contribution of MicroRNA-27b-3p to synovial fibrotic responses in knee osteoarthritis. *Arthritis Rheumatol.* **74**, 1928–1942 (2022).
27. Lietman, C. et al. Inhibition of Wnt/β-catenin signaling ameliorates osteoarthritis in a murine model of experimental osteoarthritis. *JCI Insight*. **3**, e96308–e96308 (2018).
28. Sanchez-Lopez, E., Coras, R., Torres, A., Lane, N. E. & Guma, M. Synovial inflammation in osteoarthritis progression. *Nat. Rev. Rheumatol.* **18**, 258–275 (2022).
29. Ding, L. et al. Chrysin ameliorates synovitis and fibrosis of Osteoarthritic fibroblast-like synoviocytes in rats through PERK/TXNIP/NLRP3 signaling. *Front. Pharmacol.* **14**, 1170243 (2023).
30. Perruccio, A. V. et al. Osteoarthritis year in review 2023: Epidemiology & therapy. *Osteoarthritis Cartilage* S1063-4584(23)00990–1 (2023). https://doi.org/10.1016/j.joca.2023.11.012
31. Gibbs, A. J. et al. Recommendations for the management of hip and knee osteoarthritis: A systematic review of clinical practice guidelines. *Osteoarthr. Cartil.* **31**, 1280–1292 (2023).
32. Du, S. et al. The attenuating effect of Low-Intensity pulsed ultrasound on Hypoxia-Induced rat chondrocyte damage in TMJ osteoarthritis based on TMT labeling quantitative proteomic analysis. *Front. Pharmacol.* **12**, 752734 (2021).
33. Chen, H., Wang, Z., Zhang, X. & Sun, M. Effects of low-intensity pulsed ultrasound on knee osteoarthritis: A systematic review and meta-analysis of randomized controlled trials. *Clin. Rehabil.* **36**, 1153–1169 (2022).
34. Ye, H., Li, D., Wei, X., Yu, L. & Jia, L. Focused low-intensity pulsed ultrasound alleviates osteoarthritis via restoring impaired FUNDC1-mediated mitophagy. *iScience* **26**, 107772 (2023).
35. Hu, Y. et al. Transcriptomic analyses of joint tissues during osteoarthritis development in a rat model reveal dysregulated mechanotransduction and extracellular matrix pathways. *Osteoarthr. Cartil.* **31**, 199–212 (2023).
36. Sellam, J. & Berenbaum, F. The role of synovitis in pathophysiology and clinical symptoms of osteoarthritis. *Nat. Rev. Rheumatol.* **6**, 625–635 (2010).
37. Liao, B. et al. Low-intensity pulsed ultrasound inhibits fibroblast-like synoviocyte proliferation and reduces synovial fibrosis by regulating Wnt/β-catenin signaling. *J. Orthop. Translation*. **30**, 41–50 (2021).
38. J, K. et al. Low-intensity pulsed ultrasound promotes bone morphogenic protein 9-induced osteogenesis and suppresses inhibitory effects of inflammatory cytokines on cellular responses via Rho-associated kinase 1 in human periodontal ligament fibroblasts. *J. Cell. Biochem.* **120,** 14657-14669 (2019).
39. Maglaviceanu, A., Wu, B. & Kapoor, M. Fibroblast-like synoviocytes: role in synovial fibrosis associated with osteoarthritis. *Wound Repair. Regen*. **29**, 642–649 (2021).
40. Qadri, M. M., Jay, G. D., Ostrom, R. S., Zhang, L. X. & Elsaid, K. A. cAMP attenuates TGF-β's profibrotic responses in Osteoarthritic synoviocytes: involvement of hyaluronan and PRG4. *Am. J. Physiol. Cell. Physiol.* **315**, C432–C443 (2018).
41. Ciregia, F. et al. Modulation of AVβ6 integrin in osteoarthritis-related synovitis and the interaction with VTN(381–397 a.a.) competing for TGF-β1 activation. *Exp. Mol. Med.* **53**, 210–222 (2021).
42. Li, D. et al. Lupeol protects against cardiac hypertrophy via TLR4-PI3K-Akt-NF-κB pathways. *Acta Pharmacol. Sin*. **43**, 1989–2002 (2022).
43. Wang, J. et al. Targeting PI3K/AKT signaling for treatment of idiopathic pulmonary fibrosis. *Acta Pharm. Sin B*. **12**, 18–32 (2022).
44. Wang, Y. et al. Hepatocyte Ninjurin2 promotes hepatic stellate cell activation and liver fibrosis through the IGF1R/EGR1/PDGF-BB signaling pathway. *Metabolism* **140**, 155380 (2023).
45. Cheng, K. et al. Effects of low-intensity pulsed ultrasound on integrin-FAK-PI3K/Akt mechanochemical transduction in rabbit osteoarthritis chondrocytes. *Ultrasound Med. Biol.* **40**, 1609–1618 (2014).
46. Su, W. S., Wu, C. H., Song, W. S., Chen, S. F. & Yang, F. Y. Low-intensity pulsed ultrasound ameliorates glia-mediated inflammation and neuronal damage in experimental intracerebral hemorrhage conditions. *J. Transl Med.* **21**, 565 (2023).
47. Xie, S. et al. Low-intensity pulsed ultrasound promotes the proliferation of human bone mesenchymal stem cells by activating PI3K/AKt signaling pathways. *J. Cell. Biochem.* **120**, 15823–15833 (2019).

Acknowledgements

Especially, we thank Xiao Li and Shuang Wu for their help during the experiment.

Author contributions

Q. L. was mainly involved in conceptualization, methodology, data collection, formal analysis, writing - Review & Editing. J. C. was mainly involved in validation, investigation, visualization and writing the original draft. G. L. was responsible for supervision, project administration, and funding acquisition. All authors approved the final version of the manuscript.

Funding

This study was supported by grants from the National Natural Science Foundation of China (No 82274619, 82274400).

Declarations

Competing interests

The authors declare no competing interests.

Consent for publication

Not applicable.

Additional information

Supplementary Information The online version contains supplementary material available at https://doi.org/10.1038/s41598-025-92413-x.

Correspondence and requests for materials should be addressed to G.L.

Reprints and permissions information is available at www.nature.com/reprints.

Publisher's note Springer Nature remains neutral with regard to jurisdictional claims in published maps and institutional affiliations.